



Article

In Silico Comparison of Three Different Beam Arrangements for Intensity-Modulated Proton Therapy for Postoperative Whole Pelvic Irradiation of Prostate Cancer

Emile Gogineni ^{1,2,*} , Hao Chen ², Ian K. Cruickshank, Jr. ², Andrew Koempel ¹, Aarush Gogineni ¹, Heng Li ² and Curtiland Deville, Jr. ² 

- ¹ Department of Radiation Oncology, The Ohio State University Wexner Medical Center, Columbus, OH 43210, USA; andrew.koempel@osumc.edu (A.K.); aarush.gogineni@gmail.com (A.G.)
- ² Department of Radiation Oncology and Molecular Radiation Sciences, Johns Hopkins University School of Medicine, Baltimore, MD 21205, USA; hchen142@jhmi.edu (H.C.); ian.cruickshank@bison.howard.edu (I.K.C.J.); hengli@jhmi.edu (H.L.); cdeville@jhmi.edu (C.D.J.)
- * Correspondence: emile.gogineni@osumc.edu; Tel.: +1-614-685-6808; Fax: +1-614-293-4044

Simple Summary: Proton therapy has been shown to provide dosimetric benefits in comparison with IMRT when treating prostate cancer with whole pelvis radiation; however, the optimal proton beam arrangement has yet to be established. Twenty-three post-prostatectomy patients were planned using three different beam arrangements: two-field (opposed laterals), three-field (opposed laterals inferiorly matched to a posterior–anterior beam superiorly), and four-field (opposed laterals inferiorly matched to two posterior oblique beams superiorly) arrangements. CTV coverages were similar for all plans, while the four-field plan provided the lowest doses to several metrics for bladder, bowel, sigmoid, rectum, femoral head, bone, penile bulb, and skin. The data presented herein may help inform the future delivery of whole pelvis IMPT for prostate cancer.



Citation: Gogineni, E.; Chen, H.; Cruickshank, I.K., Jr.; Koempel, A.; Gogineni, A.; Li, H.; Deville, C., Jr. In Silico Comparison of Three Different Beam Arrangements for Intensity-Modulated Proton Therapy for Postoperative Whole Pelvic Irradiation of Prostate Cancer. *Cancers* **2024**, *16*, 2702. <https://doi.org/10.3390/cancers16152702>

Academic Editors: Chia-Ho Hua and Matthew J. Krasin

Received: 15 April 2024

Revised: 17 July 2024

Accepted: 23 July 2024

Published: 30 July 2024



Copyright: © 2024 by the authors. Licensee MDPI, Basel, Switzerland. This article is an open access article distributed under the terms and conditions of the Creative Commons Attribution (CC BY) license (<https://creativecommons.org/licenses/by/4.0/>).

Abstract: Background and purpose: Proton therapy has been shown to provide dosimetric benefits in comparison with IMRT when treating prostate cancer with whole pelvis radiation; however, the optimal proton beam arrangement has yet to be established. The aim of this study was to evaluate three different intensity-modulated proton therapy (IMPT) beam arrangements when treating the prostate bed and pelvis in the postoperative setting. **Materials and Methods:** Twenty-three post-prostatectomy patients were planned using three different beam arrangements: two-field (IMPT₂B) (opposed laterals), three-field (IMPT₃B) (opposed laterals inferiorly matched to a posterior–anterior beam superiorly), and four-field (IMPT₄B) (opposed laterals inferiorly matched to two posterior oblique beams superiorly) arrangements. The prescription was 50 Gy radiobiological equivalent (GyE) to the pelvis and 70 GyE to the prostate bed. Comparisons were made using paired two-sided Wilcoxon signed-rank tests. **Results:** CTV coverages were met for all IMPT plans, with 99% of CTVs receiving $\geq 100\%$ of prescription doses. All organ at risk (OAR) objectives were met with IMPT₃B and IMPT₄B plans, while several rectum objectives were exceeded by IMPT₂B plans. IMPT₄B provided the lowest doses to OARs for the majority of analyzed outcomes, with significantly lower doses than IMPT₂B +/– IMPT₃B for bladder V30–V50 and mean dose; bowel V15–V45 and mean dose; sigmoid maximum dose; rectum V40–V72.1, maximum dose, and mean dose; femoral head V37–40 and maximum dose; bone V40 and mean dose; penile bulb mean dose; and skin maximum dose. **Conclusion:** This study is the first to compare proton beam arrangements when treating the prostate bed and pelvis. four-field plans provided better sparing of the bladder, bowel, and rectum than 2- and three-field plans. The data presented herein may help inform the future delivery of whole pelvis IMPT for prostate cancer.

Keywords: prostate cancer; radiation therapy; whole pelvis; pelvic; proton; beam arrangement; intensity-modulated proton therapy; IMPT; pencil beam; scanning beam; dosimetry; dosimetric

1. Introduction

Prostate cancer is the most common malignancy diagnosed in men in the United States and the second most common globally [1,2]. The estimated incidence of prostate cancer in 2024 in the United States is 299,010, causing an estimated 35,250 deaths [3]. Genetic, environmental, and social factors all play potential roles in the development of prostate cancer, with incidence and mortality increasingly proportionally with advancing age [2,4]. It is characterized by a heterogeneous cell population, leading to variability in the disease's natural history and prognosis [5,6]. Epithelial–mesenchymal plasticity has been hypothesized to play a role in prostate cancer's capability to metastasize and develop resistance to treatment [6].

Treatment options for localized prostate cancer include radical prostatectomy (RP) and radiation therapy (RT) with or without androgen deprivation therapy (ADT). Data from prospective studies comparing RP and RT have shown equal rates of control and survival, with RP resulting in worse incontinence and impotence, and RT leading to worse bowel and rectal irritation [7–9]. RP remains the most commonly employed treatment for prostate cancer, with biochemical failure occurring in the majority of patients with adverse pathologic features [10].

Results from multiple randomized prospective trials have proven the biochemical control benefit of postoperative radiation after RP [11–18]. Radiation Therapy Oncology Group 0534, which investigated the benefit of ADT and pelvic irradiation in patients receiving salvage RT, suggests that the addition of whole pelvis RT may provide an additional benefit over RT to the prostate bed alone [19].

Intensity-modulated photon RT (IMRT) is the most widely used radiation technique in the treatment of prostate cancer. Proton therapy has the potential to spare normal tissue in comparison with IMRT due to its rapid dose fall off beyond the target [20]. The dosimetric benefits provided by proton therapy may be more impactful when treating the pelvic lymph nodes due to the large volumes receiving radiation. While prospective data proving benefits are currently lacking, protons have the potential to decrease toxicity, improve quality of life, and reduce rates of second malignancy after treatment.

Intensity-modulated proton therapy (IMPT) using two opposed lateral beams has been shown to reduce the dose to the bladder, bowel, and rectum in comparison to IMRT when treating intact prostate and pelvic nodal fields while providing adequate clinical target volume (CTV) coverage in a dosimetric analysis by Whitaker et al., in which a simultaneous integrated boost was utilized to treat the nodal volume to 45 Gy and the prostate to 67.5 Gy, all in 25 fractions [21]. A single institution, retrospective matched comparison by Santos et al. found that proton therapy to the prostate bed only was superior at reducing the volumes of bladder and rectum receiving 10% to 40% of the dose compared to IMRT [22]. IMPT has also been shown to reduce the dose to organs at risk (OARs) when treating the whole pelvis postoperatively [23].

While IMPT provides dosimetric benefits in comparison with IMRT, the optimal proton beam arrangement has yet to be established when treating with whole pelvis RT. The aim of this study was to evaluate dosimetric differences between three different beam arrangements when treating the prostate bed and pelvic lymph nodes with IMPT in the postoperative setting.

2. Materials and Methods

After obtaining approval from our institutional review board, we identified 23 patients with prostate cancer who had undergone initial RP and were then treated with IMPT in the postoperative setting between July 2020 and August 2020. Patients with gross lymphadenopathy and/or distant metastases seen on imaging and those who had received previous irradiation were excluded from analysis.

2.1. Simulation

Patients were simulated supine with a full bladder and an empty rectum with a rectal balloon in place. Magnetic resonance imaging (MRI) simulation was obtained immediately following computed tomography (CT) simulation.

2.2. Volume Delineation

All CTV and OAR contours were delineated by the attending radiation oncologist in the RayStation treatment planning system (RaySearch Laboratories, Stockholm, Sweden). The CTVs included the pelvic lymph nodes (CTV1) and the postoperative prostate bed (CTV2), delineated according to the Radiation Therapy Oncology Group 0534 protocol [19] and the 2021 NRG Oncology Consensus Pelvic Lymph Node Atlas [24]. CTV1 was combined with CTV2 to create CTV_50.

Planning target volumes (PTVs) were created from CTV expansions according to our institutional protocol. These PTVs were created for evaluation purposes only, as has been described in previous studies, and were not used in planning [25–27]. Thus, expansions from CTV to PTV were not identical to the margins used for robust planning. PTV1 was generated using a 5 mm expansion in all directions from CTV1. PTV2 was generated using a 6 mm cranial and caudal expansion from CTV2, and a 5 mm radial expansion from CTV2. PTV_70_Eval was created using a 5 mm lateral margin from PTV_70 to account for range uncertainty, including relative bone thickness change due to prostate interfraction motion. PTV1 was combined with PTV2 to create PTV_50.

Contoured OARs included the bladder, bowel cavity, sigmoid, rectum, femoral heads, penile bulb, bone, and skin. The OAR 'Rectum (in-field)' included the portion of the rectum 10 mm superior and inferior to the CTV, while the OAR 'Rectum (anatomic)' included the entire anatomic rectum. An additional OAR 'Bladderless_CTV' was delineated, which included the entire bladder excluding any overlapping CTV. The OAR 'Bone' was generated as a surrogate for bone marrow dose, which was limited to bones 10 mm superior and inferior to the CTV.

2.3. Treatment Planning

CTV_50 was prescribed a dose of 50 Gy radiobiological equivalent (GyE) over 25 fractions, which was followed by an additional 10 fraction 20 GyE cone down to CTV2 = CTV_70 to a total of 70 GyE over 35 fractions. A relative biological effectiveness (RBE) dose of 1.1 was used for proton equivalent doses.

Three sets of IMPT plans were prepared for each patient with predefined CTV and OAR dose-volume histogram (DVH) objectives as outlined in Table 1. These plans were created using 3 different beam arrangements: 2-field (IMPT₂B) (opposed laterals), 3-field (IMPT₃B) (opposed laterals inferiorly matched to a posterior–anterior [PA] beam superiorly), and 4-field (IMPT₄B) (opposed laterals inferiorly matched to 2 posterior oblique [PO] beams superiorly) arrangements. PO beams were delivered 25–35 degrees off from the PA direction. For IMPT₃B and IMPT₄B, the PA and PO beams were arranged to cover the superior portion of the target until the base of the prostate and then fade out using a gradient match. The lateral beams began superiorly where there was no bowel lateral to the CTV and covered the entirety of the remaining inferior portion of the target optimized with a single-field optimization (SFO) technique. The dose in the overlapped regions for lateral beams and PA/PO beams was gradient matched in the superior and inferior directions. Figure 1 depicts an example of the dose-color-wash for each plan.

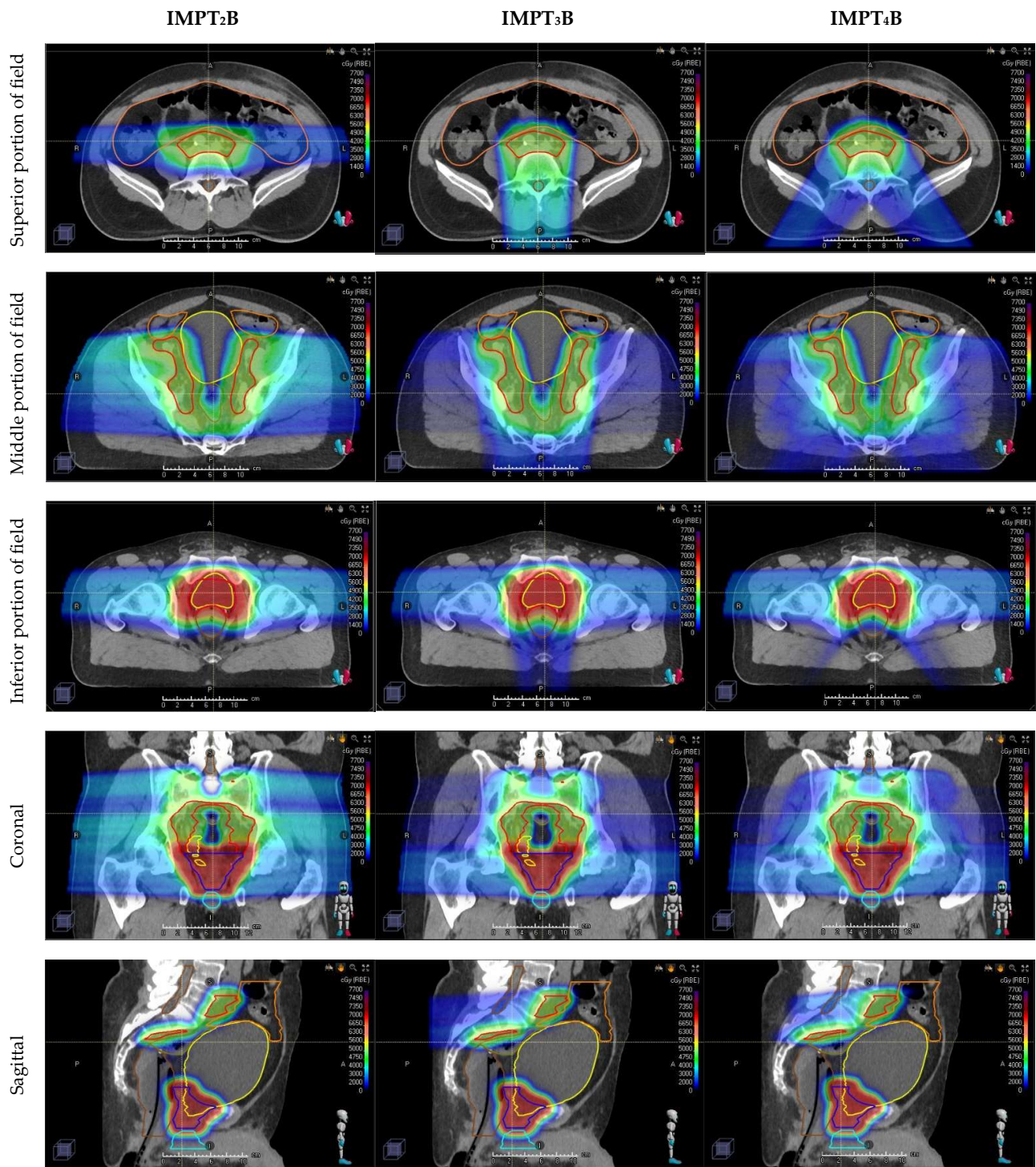


Figure 1. Representative dose-color-wash images in axial (top three rows), coronal (4th row), and sagittal (bottom row) comparing three different proton beam arrangements, with the dose increasing as the color ranges from blue to green to red. Axial images are divided into superior (1st row), middle (2nd row), and inferior (3rd row) portions of the target. Compared plans include 2-field: IMPT₂B (left), 3-field: IMPT₃B (middle), and 4-field: IMPT₄B (right) plans.

Table 1. Comparative dosimetric outcomes for IMPT 2-, 3-, and 4-field plans. Mean and standard deviation values are provided as percentages or cubic centimeters (as denoted in the column labeled “Clinical Goal”) for volumetric endpoints and as GyE for mean and maximum dose endpoints.

Target/OAR	Clinical Goal	IMPT ₂ B		IMPT ₃ B		IMPT ₄ B		2B vs 3B	p-Value	
		Mean	St-Dev	Mean	St-Dev	Mean	St-Dev		2B vs 4B	3B vs 4B
CTV_50	V 49.0 GyE > 98.0%	100	0.1	100	0.0	100	0.0	0.348	0.215	0.162
	V 50.0 GyE > 98.0%	99.6	0.6	99.6	0.6	99.8	0.2	0.864	0.117	0.136
CTV_70	V 68.6 GyE > 99.0%	100	0.0	100	0.0	100	0.0	N/A	N/A	N/A
	V 70.0 GyE > 99.0%	99.8	0.4	99.8	0.5	99.7	0.5	0.519	0.282	0.375
Bladder	V 30.0 GyE < 50.0%	46.5	9.6	45.8	10.6	43.7	9.2	0.337	<0.001	0.004
	V 45.0 GyE < 40.0%	37.7	9.5	37.7	10.0	36.3	9.1	0.887	<0.001	0.001
	V 50.0 GyE < 35.0%	33.8	9.6	34.1	9.8	33.3	9.4	0.274	0.129	0.002
	V 65.0 GyE < 20.0%	25.5	9.1	25.5	9.2	25.4	9.0	0.973	0.933	0.927
	V 70.0 GyE < 15.0%	21.3	8.4	21.2	8.4	22.7	8.6	0.123	<0.001	<0.001
	Mean Dose (GyE)	31.3	6.4	31.0	6.8	29.9	6.4	0.453	<0.001	0.003
Bladderless_CTV	V 30.0 GyE < 50.0%	36.9	7.6	36.2	8.2	33.7	6.5	0.364	<0.001	0.003
	V 45.0 GyE < 40.0%	26.5	6.0	26.6	6.5	24.9	5.4	0.829	<0.001	0.001
	V 50.0 GyE < 35.0%	21.9	5.5	22.3	5.8	21.4	5.1	0.227	0.145	0.003
	V 65.0 GyE < 20.0%	12.0	3.8	12.0	3.9	12.0	3.7	1.000	0.986	0.979
	V 70.0 GyE < 15.0%	7.1	2.4	6.9	2.5	8.7	2.9	0.123	<0.001	<0.001
	D 0.03 cm ³ < 73.5 GyE	72.5	0.6	72.4	0.5	73.0	0.3	0.036	0.002	<0.001
	Mean Dose (GyE)	24.1	4.4	23.9	4.8	22.6	4.1	0.494	<0.001	0.002
Bowel Cavity	V 15.0 GyE < 830.0 cm ³	530.0	202.7	219.8	92.8	200.0	83.7	<0.001	<0.001	<0.001
	V 30.0 GyE < 300.0 cm ³	170.1	71.7	140.8	61.1	131.4	57.9	<0.001	<0.001	0.002
	V 40.0 GyE < 30.0%	6.2	4.1	5.2	3.6	4.9	2.9	<0.001	<0.001	0.086
	V 45.0 GyE < 195.0 cm ³	81.2	37.6	68.8	32.2	70.5	33.9	<0.001	<0.001	0.298
	V 55.0 GyE < 20.0 cm ³	0.7	2.0	0.7	2.1	0.8	2.2	0.446	0.262	0.510
	V 60.0 GyE < 5.0 cm ³	0.4	1.3	0.4	1.4	0.5	1.5	0.445	0.224	0.489
	Mean Dose (GyE)	8.8	3.3	4.9	3.1	4.6	2.6	<0.001	<0.001	0.013
Sigmoid	D 0.03 cm ³ < 66.0 GyE	59.0	7.1	58.8	6.9	56.7	7.0	0.599	<0.001	<0.001
Rectum (anatomic)	V 40.0 GyE < 40.0%	33.7	8.2	34.7	9.7	28.9	6.8	0.160	<0.001	<0.001
	V 50.0 GyE < 30.0%	26.8	7.3	26.9	8.4	22.3	5.8	0.822	<0.001	<0.001
	V 60.0 GyE < 20.0%	19.5	6.0	19.0	6.5	15.8	4.6	0.209	<0.001	<0.001
	V 70.0 GyE < 10.0%	5.5	2.2	4.7	2.0	4.0	1.9	<0.001	<0.001	0.009
	V 72.1 GyE < 0.5 cm ³	0.1	0.2	0.1	0.2	0.0	0.0	0.102	0.038	0.266
	D 0.03 cm ³ < 72.1 GyE	72.1	0.6	71.6	0.6	71.2	0.3	<0.001	<0.001	0.005
	Mean Dose (GyE)	27.3	5.2	29.4	6.0	24.6	4.5	0.001	<0.001	<0.001
Rectum (in-field)	V 40.0 GyE < 40.0%	34.7	8.8	35.8	10.4	30.2	7.4	0.162	<0.001	<0.001
	V 50.0 GyE < 30.0%	27.7	7.8	27.8	9.0	23.3	6.3	0.825	<0.001	<0.001
	V 60.0 GyE < 20.0%	20.2	6.4	19.7	7.0	16.6	4.9	0.204	<0.001	<0.001
	V 70.0 GyE < 10.0%	5.7	2.2	4.8	2.0	4.1	1.9	0.001	<0.001	0.009
	V 72.1 GyE < 0.5 cm ³	0.1	0.2	0.1	0.2	0.0	0.0	0.114	0.039	0.270
	D 0.03 cm ³ < 72.1 GyE	72.1	0.6	71.6	0.6	71.2	0.3	<0.001	<0.001	0.005
	Mean Dose (GyE)	28.1	5.5	30.2	6.3	25.6	4.8	0.001	<0.001	<0.001
Left Femoral Head	V 37.0 GyE < 50.0%	0.9	1.3	0.1	0.3	0.1	0.1	0.004	0.002	0.470
	V 40.0 GyE < 40.0%	0.2	0.3	0.0	0.1	0.0	0.1	0.016	0.003	0.788
	V 50.0 GyE < 10.0%	0.0	0.0	0.0	0.0	0.0	0.0	N/A	N/A	N/A
	D 0.03 cm ³ < 53.0 GyE	40.2	3.2	35.6	3.4	34.2	3.9	<0.001	<0.001	0.015
Right Femoral Head	V 37.0 GyE < 50.0%	1.0	1.3	0.2	0.7	0.0	0.1	0.009	0.002	0.312
	V 40.0 GyE < 40.0%	0.1	0.2	0.1	0.3	0.0	0.0	0.546	0.017	0.361
	V 50.0 GyE < 10.0%	0.0	0.0	0.0	0.0	0.0	0.0	N/A	N/A	N/A
	D 0.03 cm ³ < 53.0 GyE	40.3	3.3	36.1	3.5	34.4	4.1	<0.001	<0.001	0.006
Bone	V 10.0 GyE < 90.0%	73.5	5.1	82.4	5.0	83.4	3.4	<0.001	<0.001	0.027
	V 40.0 GyE < 37.0%	20.8	4.9	21.8	3.9	19.6	3.3	0.163	0.060	0.000
	Mean Dose (GyE)	26.0	2.5	27.5	2.1	26.6	1.9	0.001	0.038	0.001

Table 1. Cont.

Target/OAR	Clinical Goal	IMPT ₂ B		IMPT ₃ B		IMPT ₄ B		p-Value		
		Mean	St-Dev	Mean	St-Dev	Mean	St-Dev	_{2B vs 3B}	_{2B vs 4B}	_{3B vs 4B}
Penile Bulb	Mean < 52.5 GyE	23.6	6.2	23.7	7.3	22.0	6.6	0.848	0.003	<0.001
Skin	D 0.03 cm ³ < 56.0 GyE	36.4	2.4	36.8	1.5	31.0	1.7	0.652	<0.001	<0.001

Abbreviations: IMPT: intensity-modulated proton therapy, OAR: organ at risk, ₂B: 2-field plan, ₃B: 3-field plan, ₄B: 4-field plan, St-Dev: standard deviation, CTV: clinical target volume, GyE: radiobiological Gy equivalent.

Plans differed in how the dose was delivered to the superior portion of the field, in which beams were arranged with 2 opposed lateral beams for IMPT₂B, a single posterior–anterior beam for IMPT₃B, and 2 posterior oblique beams for IMPT₄B. These beam arrangements covered the target until the base of the prostate, then faded out using a gradient match to the inferior portion of the field, which was covered by opposed laterals for all 3 plans.

As shown in the axial images (1st row), the opposed lateral beams range directly through the bowel in the superior portion of the field, which correlates with higher doses to the bowel with the IMPT₂B plans seen in Table 1 and Figure 2C. Figures from the inferior portion of the field (3rd row) depict the increased conformality of the dose deposited posterior to the prostate with IMPT₄B plans, correlating with the lower rectal doses shown in Table 1 and Figure 2E,F.

Plans were generated by multiple proton-specialist dosimetrists using the RayStation treatment planning system. Proton plans were created with pencil beam scanning (IMPT) using inverse optimization with robustness with a setup uncertainty of 3 mm and a range uncertainty of 3.5% using fast graphics processing units (GPU) Monte Carlo optimization. The goal was to cover PTV_70_Eval with 95% of the prescription isodose in both lateral directions to evaluate for the robustness for range uncertainty, daily skin surface uncertainty, and the daily related motion to bone anatomy.

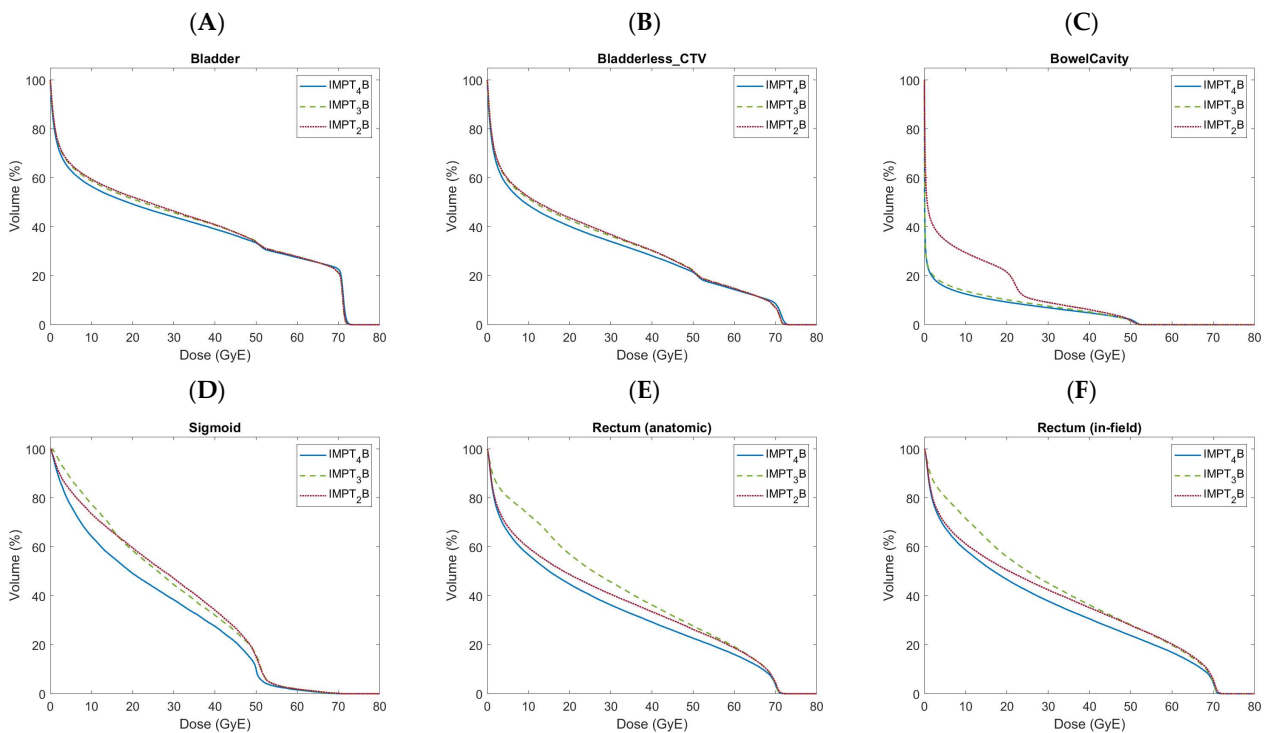


Figure 2. Cont.

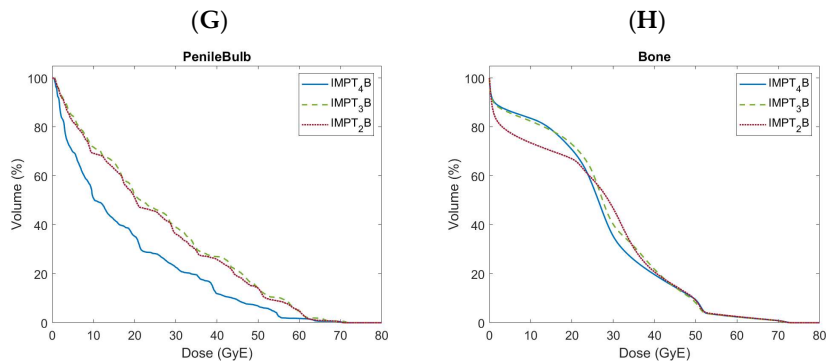


Figure 2. Doses to organs at risk shown over the entire dose-volume histogram comparing 2- (IMPT₂B), 3- (IMPT₃B), and 4-field (IMPT₄B) proton beam arrangements, including the bladder (A), bladderless_CTV (B), bowel (C), sigmoid (D), anatomic rectum (E), in-field rectum (F), penile bulb (G), and bone (H).

2.4. Statistical Analysis

The volumetric percentage of CTVs and OARs along the entire DVH were evaluated. Comparative maximum and mean OAR doses were also assessed. The paired 2-sided Wilcoxon signed-rank test was used to compare the plans with $p < 0.05$ considered statistical significance. Statistical analyses were performed using Matlab R2024a (MathWorks, Natick, MA, USA) and Microsoft Office LTSC Professional Plus 2021 Excel (Microsoft, Redmond, WA, USA).

3. Results

Table 1 provides comparative values for target coverage and the doses to OARs. Comparative DVH's for OARs are shown in Figure 2A–H.

3.1. Target Coverage

CTV₅₀ and CTV₇₀ coverages were met for all IMPT plans, with 99% of CTVs receiving $\geq 100\%$ of prescription doses. CTV coverages were numerically highest with IMPT₄B plans for all objectives except the volume of CTV₇₀ receiving 70.0 GyE, which was highest with IMPT₂B plans (not statistically significant). There were no significant differences in CTV coverage between plans.

3.2. Organ at Risk Objectives

The volume of in-field rectum receiving 60.0 GyE exceeded objectives for IMPT₂B plans. The maximum dose to both the anatomic and the in-field rectum exceeded objectives for IMPT₂B plans. All OAR objectives were met for IMPT₃B and IMPT₄B plans.

3.3. Genitourinary Organs at Risk

Volumes of the irradiated bladder (Figure 2A) and bladderless_CTV (Figure 2B) were numerically lowest with IMPT₄B plans for all objectives except for volumes of the bladder and bladderless_CTV receiving 70.0 GyE and the maximum dose to bladderless_CTV, which were lowest with IMPT₃B plans. Volumes of the bladder and bladderless_CTV receiving 30.0 and 45.0 GyE were significantly lower with IMPT₄B plans than with both IMPT₂B and IMPT₃B plans, while volumes receiving 50.0 GyE were significantly lower with IMPT₄B plans than with IMPT₃B plans. Volumes of the bladder and bladderless_CTV receiving 70.0 GyE and maximum doses were significantly higher with IMPT₄B plans than those with both IMPT₂B and IMPT₃B plans. Mean doses to the bladder and bladderless_CTV were numerically lowest with IMPT₄B plans, with significantly lower mean doses than those with IMPT₂B and IMPT₃B plans.

3.4. Gastrointestinal Organs at Risk

Volumes of the irradiated bowel cavity (Figure 2C) were numerically lowest with IMPT₄B plans for all objectives < 45.0 GyE and lowest with IMPT₃B plans for objectives ≥ 45.0 GyE. Volumes of the bowel cavity receiving 15.0 and 30.0 GyE were significantly lower with IMPT₃B plans than with IMPT₂B plans and significantly lower with IMPT₄B plans than with both IMPT₂B and IMPT₃B plans. Volumes of the bowel cavity receiving 40.0 and 45.0 GyE were significantly higher with IMPT₂B plans than with both IMPT₃B plans and IMPT₄B. The mean dose to the bowel was numerically lowest with IMPT₄B plans, with a significantly lower mean dose than IMPT₂B and IMPT₃B plans. IMPT₃B plans also had a significantly lower mean dose to the bowel than IMPT₂B plans.

The maximum dose to the sigmoid (Figure 2D) was numerically lowest with IMPT₄B plans, with significantly lower maximum doses than IMPT₂B and IMPT₃B plans.

Volumes of the irradiated anatomic (Figure 2E) and the in-field rectum (Figure 2F) were numerically lowest with IMPT₄B plans for all doses. Volumes of the anatomic and the in-field rectum receiving 40.0, 50.0, 60.0, and 70.0 GyE were significantly lower with IMPT₄B plans than with both IMPT₂B and IMPT₃B plans. Volumes of the anatomic and the in-field rectum receiving 70.0 GyE were also significantly lower with IMPT₃B plans than with IMPT₂B plans. Volumes of the anatomic and the in-field rectum receiving 72.1 GyE were significantly lower with IMPT₄B plans than IMPT₂B plans. Maximum doses to the anatomic and the in-field rectum were significantly lower with IMPT₄B plans than with both IMPT₂B and IMPT₃B plans, while IMPT₃B plans also had significantly lower maximum doses than IMPT₂B plans. Mean doses to the anatomic and the in-field rectum were numerically lowest with IMPT₄B plans, with significantly lower mean doses than those with IMPT₂B and IMPT₃B plans. IMPT₃B plans also had significantly higher mean doses to the anatomic and the in-field rectum than IMPT₂B plans.

3.5. Bony Organs at Risk

Volumes of the irradiated left and right femoral heads were numerically lowest with IMPT₄B plans for all doses. Volumes of each femoral head receiving 37.0 and 40.0 GyE were significantly lower with IMPT₄B plans than with IMPT₂B plans. The maximum dose to each femoral head was significantly lower with IMPT₄B plans than with both IMPT₂B and IMPT₃B plans.

The volume of bone (Figure 2H) receiving 10.0 GyE was numerically lowest with IMPT₂B plans and was significantly lower than that with both IMPT₃B and IMPT₄B plans. The volume of bone receiving 40.0 GyE was numerically lowest with IMPT₄B plans and was significantly lower than that with IMPT₃B plans. The mean dose to bone was numerically lowest with IMPT₂B plans, with a significantly lower mean dose than with IMPT₃B and IMPT₄B plans. IMPT₄B plans also had a significantly lower mean dose to bone than IMPT₃B plans.

3.6. Other Organs at Risk

The mean dose to the penile bulb (Figure 2G) was numerically lowest with IMPT₄B plans, with a significantly lower mean dose than with IMPT₂B and IMPT₃B plans.

The maximum dose to skin was numerically lowest with IMPT₄B plans and was significantly lower than with both IMPT₂B and IMPT₃B plans.

4. Discussion

This is the first study to our knowledge comparing proton beam arrangements when treating the prostate bed and elective pelvic lymph nodes in the postoperative setting. We found that the four-field IMPT beam arrangement showed the greatest reductions in low-to-intermediate doses to OARs, particularly in the bowel and rectum, compared to the two- and three-field arrangement. IMPT₄B also provided the lowest mean dose to the bladder, bowel, rectum, and penile bulb while maintaining similar or better target coverage.

4.1. Beam Arrangements

There has been limited data published to date evaluating differences between varying proton beam arrangements when treating the pelvic lymph nodes with IMPT. Butala et al. suggested that the treatment of pelvic lymph nodes using a three-field approach with a posterior field matched inferiorly with opposed lateral beams to treat the prostate improves OAR sparing in comparison with a plan solely utilizing opposed lateral beams to treat both the prostate and the whole pelvis. They did not address the use of a four-field beam arrangement for proton irradiation using PO beams to treat the pelvis, as is carried out in the study presented herein.

Regarding the treatment of intact prostate cancer and the prostate target volume, Tang et al. compared three different arrangements of proton beams, including equally weighted bilateral fields, a single straight anterior field, and two equally weighted anterior oblique (AO) fields. They found that AO fields decreased the dose to the anterior rectal wall and femoral heads in comparison with lateral fields [28]. Underwood et al. compared four treatment plans, including photon IMRT, passively scattered opposed lateral proton beams, passively scattered AO proton beams, and AO IMPT [29]. They found that plans utilizing AO beam arrangements typically did not meet both tumor and OAR constraints, often resulting in substantial hotspots within the rectum. Both of these studies focused on the treatment of the prostate alone and did not evaluate patients receiving whole pelvis radiation therapy (WPRT), nor did they include the three- and four-field beam arrangements used in our analysis.

A study from the University of Florida by Chera et al. compared photon IMRT to a four-field proton plan to the intact prostate, seminal vesicles, and pelvic lymph nodes [30]. They used opposed lateral fields to treat the prostate and four fields to treat the pelvis, including two lateral and two PO beams. Despite the use of double-scattered proton beams with uniform intensities, they did find a reduction in the dose to OARs using this arrangement in comparison with IMRT. However, they did not utilize modern proton scanning beam technology and did not compare this beam arrangement to others, such as the IMPT₂B, IMPT₃B, and IMPT₄B comparison described in our cohort.

4.2. Correlation between Dosimetric Outcomes and Toxicity

There are no prospective proton therapy studies to date assessing whether these dosimetric differences between beam arrangements translate to reductions in toxicity and improved quality of life. However, gastrointestinal (GI) toxicity has been shown to correlate with the volume of the irradiated rectum. Kuban et al. suggested that the volumes of the rectum receiving low doses of radiation may be even more significant in predicting rectal morbidity [31–34]. Our study shows a reduction in the volume of the rectum receiving doses of 40, 50, 60, and 70 GyE with the IMPT₄B arrangement (see Table 1 and Figure 2E,F). It also demonstrates a reduction in the volume of the bowel receiving 45 GyE in the IMPT₃B and IMPT₄B plans and the lowest volume of the bowel receiving 15 GyE in the IMPT₄B plan (see Table 1 and Figure 2C), which have both been shown to be predictive of grade ≥ 3 acute GI toxicity [35].

Bryant et al. showed that grade 3 genitourinary (GU) toxicity was significantly associated with bladder V30 on univariate (hazard ratio [HR]: 0.4) and multivariate analysis (HR: 0.5) [36]. We found that bladder and bladderless_CTV V30 were lowest with the IMPT₄B plan, which was significantly lower than that of IMPT₂B and IMPT₃B plans (see Table 1 and Figure 2A,B).

4.3. Robustness

Movement-induced dose reduction occurs significantly more with the proton irradiation of the prostate using opposed lateral beams when compared to photon irradiation [37–39]. This is due to variations in femur rotation, the thickness of subcutaneous adipose tissue, and changes in bladder and bowel filling. Yoon et al. showed that a lateral shift of 6 mm decreased coverage by 9% for a proton plan when treating with opposed lateral beams, as

opposed to only 1% for a photon IMRT plan [38]. These sensitivities of coverage for proton irradiation can be mitigated by the use of IMPT with appropriate planning strategies and minimizing motion with serial cone-beam CT imaging and immobilization devices such as a rectal balloon [40,41].

The effect of beam arrangement on plan robustness is multifactorial. For example, the majority of patients have a slight indent at midline in the posterior lumbar region. Thus, a small lateral shift could have a greater effect on the PA beam used in the IMPT_{3B} plan than on the PO beams used in the IMPT_{4B} plan, given that the PA beam traverses directly through this indent. On the other hand, the larger number of beams used in the IMPT_{4B} plan increases the time required to deliver each fraction and could affect the robustness of the plan due to the potential that the patient could move. Given the complexity of this concept and the difficulty accounting for each of these variables, we did not perform a formal comparison of robustness between beam arrangements.

4.4. Limitations

This study is limited by the number of patients included. While 23 patients may not provide a robust cohort to make strong conclusions when analyzing clinical outcomes in a retrospective study, it is significantly larger than most dosimetric studies, which typically do not include more than 10 patients [21,23,30,42–45]. All patients underwent simulation and treatment planning with rectal balloons in place. Correspondingly, conclusions made from our study should not be extrapolated to settings in which rectal balloons are not used.

Another limitation of this study was the lack of proof that the dosimetric outcomes found will correlate directly with quality of life and toxicity. However, further optimization of beam arrangement and delivery allowing increasing plan conformality has the potential to maximize the benefits provided by the unique physical properties of proton irradiation. This may lead to clearer clinical benefits over time. Our group is conducting analyses using normal tissue complication probability models in order to assess whether the dosimetric findings from our study may predict differences in toxicity and quality of life. Ultimately, clinical data are necessary to understand differences in patient outcomes.

5. Conclusions

This study is the first to provide a dosimetric comparison of proton beam arrangements when treating the prostate bed and pelvic lymph nodes. Mean and low-to-intermediate doses to organs at risk were lower with the four-field plan than with the two- and three-field plans, particularly for the bladder, bowel, and rectum. The data presented herein may help inform the future delivery of proton therapy for prostate cancer in the postoperative setting.

Author Contributions: Conceptualization, E.G. and C.D.J.; data curation, I.K.C.J.; formal analysis, H.C.; investigation, E.G.; methodology, E.G. and C.D.J.; resources, E.G.; supervision, E.G. and C.D.J.; validation, E.G.; visualization, E.G. and C.D.J.; writing—original draft, E.G., A.G. and C.D.J.; writing—review and editing, E.G., H.C., I.K.C.J., A.K., A.G., H.L. and C.D.J. All authors have read and agreed to the published version of the manuscript.

Funding: This research received no external funding.

Institutional Review Board Statement: The study was conducted in accordance with the Declaration of Helsinki and approved by the Institutional Review Boards of Johns Hopkins University: #IRB00228501.

Informed Consent Statement: Patient consent was waived, as no identifiable information was included.

Data Availability Statement: Research data are stored in an institutional repository and will be shared upon request to the corresponding author.

Conflicts of Interest: The authors declare no conflicts of interest.

Abbreviations

RP	Radical prostatectomy
RT	Radiation therapy
ADT	Androgen deprivation therapy
IMRT	Intensity-modulated photon radiation therapy
IMPT	Intensity-modulated proton therapy
CTV	Clinical target volume
OAR	Organ at risk
MRI	Magnetic resonance imaging
CT	Computed tomography
PTV	Planning target volume
GyE	Gy radiobiologic equivalent
RBE	Relative biological effectiveness
DVH	Dose-volume histogram
IMPT ₂ B	two-field IMPT beam arrangement using opposed laterals
IMPT ₃ B	three-field IMPT beam arrangement using opposed laterals inferiorly matched to a Posterior–anterior beam superiorly
PA	Posterior–anterior
IMPT ₄ B	four-field IMPT beam arrangement using opposed laterals inferiorly matched to 2 Posterior oblique beams superiorly
PO	Posterior oblique
SFO	Single-field optimization
GPU	Graphics processing units
AO	Anterior oblique
WPRT	Whole pelvis radiation therapy
GI	Gastrointestinal
GU	Genitourinary
HR	Hazard ratio

References

1. American Cancer Society. Cancer Facts and Figures 2021. Available online: <https://www.cancer.org/content/dam/cancer-org/research/cancer-facts-and-statistics/annual-cancer-facts-and-figures/2021/cancer-facts-and-figures-2021.pdf> (accessed on 11 October 2021).
2. Rawla, P. Epidemiology of Prostate Cancer. *World J. Oncol.* **2019**, *10*, 63–89. [[CrossRef](#)]
3. Siegel, R.L.; Giaquinto, A.N.; Jemal, A. Cancer statistics, 2024. *CA Cancer J. Clin.* **2024**, *74*, 12–49. [[CrossRef](#)] [[PubMed](#)]
4. Torre, L.A.; Siegel, R.L.; Ward, E.M.; Jemal, A. Global Cancer Incidence and Mortality Rates and Trends—An Update. *Cancer Epidemiol. Biomark. Prev.* **2016**, *25*, 16–27. [[CrossRef](#)]
5. Tzelepi, V. Prostate Cancer: Pathophysiology, Pathology and Therapy. *Cancers* **2022**, *15*, 281. [[CrossRef](#)] [[PubMed](#)]
6. Papanikolaou, S.; Vourda, A.; Syggelos, S.; Gyftopoulos, K. Cell Plasticity and Prostate Cancer: The Role of Epithelial-Mesenchymal Transition in Tumor Progression, Invasion, Metastasis and Cancer Therapy Resistance. *Cancers* **2021**, *13*, 2795. [[CrossRef](#)]
7. Sanda, M.G.; Dunn, R.L.; Michalski, J.; Sandler, H.M.; Northouse, L.; Hembroff, L.; Lin, X.; Greenfield, T.K.; Litwin, M.S.; Saigal, C.S.; et al. Quality of life and satisfaction with outcome among prostate-cancer survivors. *N. Engl. J. Med.* **2008**, *358*, 1250–1261. [[CrossRef](#)]
8. Donovan, J.L.; Hamdy, F.C.; Lane, J.A.; Mason, M.; Metcalfe, C.; Walsh, E.; Blazeby, J.M.; Peters, T.J.; Holding, P.; Bonnington, S.; et al. Patient-Reported Outcomes after Monitoring, Surgery, or Radiotherapy for Prostate Cancer. *N. Engl. J. Med.* **2016**, *375*, 1425–1437. [[CrossRef](#)]
9. Hamdy, F.C.; Donovan, J.L.; Lane, J.A.; Mason, M.; Metcalfe, C.; Holding, P.; Davis, M.; Peters, T.J.; Turner, E.L.; Martin, R.M.; et al. 10-Year Outcomes after Monitoring, Surgery, or Radiotherapy for Localized Prostate Cancer. *N. Engl. J. Med.* **2016**, *375*, 1415–1424. [[CrossRef](#)] [[PubMed](#)]
10. Tendulkar, R.D.; Agrawal, S.; Gao, T.; Efstathiou, J.A.; Pisansky, T.M.; Michalski, J.M.; Koontz, B.F.; Hamstra, D.A.; Feng, F.Y.; Liauw, S.L.; et al. Contemporary Update of a Multi-Institutional Predictive Nomogram for Salvage Radiotherapy After Radical Prostatectomy. *J. Clin. Oncol.* **2016**, *34*, 3648–3654. [[CrossRef](#)]
11. Thompson, I.M.; Tangen, C.M.; Paradelo, J.; Lucia, M.S.; Miller, G.; Troyer, D.; Messing, E.; Forman, J.; Chin, J.; Swanson, G.; et al. Adjuvant radiotherapy for pathologically advanced prostate cancer: A randomized clinical trial. *JAMA* **2006**, *296*, 2329–2335. [[CrossRef](#)]

12. Thompson, I.M.; Tangen, C.M.; Paradelo, J.; Lucia, M.S.; Miller, G.; Troyer, D.; Messing, E.; Forman, J.; Chin, J.; Swanson, G.; et al. Adjuvant radiotherapy for pathological T3N0M0 prostate cancer significantly reduces risk of metastases and improves survival: Long-term followup of a randomized clinical trial. *J. Urol.* **2009**, *181*, 956–962. [[CrossRef](#)] [[PubMed](#)]
13. Bolla, M.; van Poppel, H.; Collette, L.; van Cangh, P.; Vekemans, K.; Da Pozzo, L.; de Reijke, T.M.; Verbaeys, A.; Bosset, J.F.; van Velthoven, R.; et al. Postoperative radiotherapy after radical prostatectomy: A randomised controlled trial (EORTC trial 22911). *Lancet* **2005**, *366*, 572–578. [[CrossRef](#)] [[PubMed](#)]
14. Bolla, M.; van Poppel, H.; Tombal, B.; Vekemans, K.; Da Pozzo, L.; de Reijke, T.M.; Verbaeys, A.; Bosset, J.F.; van Velthoven, R.; Colombel, M.; et al. Postoperative radiotherapy after radical prostatectomy for high-risk prostate cancer: Long-term results of a randomised controlled trial (EORTC trial 22911). *Lancet* **2012**, *380*, 2018–2027. [[CrossRef](#)] [[PubMed](#)]
15. Wiegel, T.; Bottke, D.; Steiner, U.; Siegmann, A.; Golz, R.; Störkel, S.; Willich, N.; Semjonow, A.; Souchon, R.; Stöckle, M.; et al. Phase III postoperative adjuvant radiotherapy after radical prostatectomy compared with radical prostatectomy alone in pT3 prostate cancer with postoperative undetectable prostate-specific antigen: ARO 96-02/AUO AP 09/95. *J. Clin. Oncol.* **2009**, *27*, 2924–2930. [[CrossRef](#)] [[PubMed](#)]
16. Wiegel, T.; Bartkowiak, D.; Bottke, D.; Bronner, C.; Steiner, U.; Siegmann, A.; Golz, R.; Störkel, S.; Willich, N.; Semjonow, A.; et al. Adjuvant radiotherapy versus wait-and-see after radical prostatectomy: 10-year follow-up of the ARO 96-02/AUO AP 09/95 trial. *Eur. Urol.* **2014**, *66*, 243–250. [[CrossRef](#)] [[PubMed](#)]
17. Morgan, S.C.; Waldron, T.S.; Eapen, L.; Mayhew, L.A.; Winkquist, E.; Lukka, H.; Genitourinary Cancer Disease Site Group of the Cancer Care Ontario Program in Evidence-based Care. Adjuvant radiotherapy following radical prostatectomy for pathologic T3 or margin-positive prostate cancer: A systematic review and meta-analysis. *Radiother. Oncol.* **2008**, *88*, 1–9. [[CrossRef](#)] [[PubMed](#)]
18. Daly, T.; Hickey, B.E.; Lehman, M.; Francis, D.P.; See, A.M. Adjuvant radiotherapy following radical prostatectomy for prostate cancer. *Cochrane Database Syst. Rev.* **2011**, CD007234. [[CrossRef](#)] [[PubMed](#)]
19. Pollack, A.; Karrison, T.G.; Balogh, A.G.; Gomella, L.G.; Low, D.A.; Bruner, D.W.; Wefel, J.S.; Martin, A.G.; Michalski, J.M.; Angyalfi, S.J.; et al. The addition of androgen deprivation therapy and pelvic lymph node treatment to prostate bed salvage radiotherapy (NRG Oncology/RTOG 0534 SPPORT): An international, multicentre, randomised phase 3 trial. *Lancet* **2022**, *399*, 1886–1901. [[CrossRef](#)] [[PubMed](#)]
20. Wilson, R.R. Radiological use of fast protons. *Radiology* **1946**, *47*, 487–491. [[CrossRef](#)] [[PubMed](#)]
21. Whitaker, T.J.; Routman, D.M.; Schultz, H.; Harmsen, W.S.; Corbin, K.S.; Wong, W.W.; Choo, R. IMPT versus VMAT for Pelvic Nodal Irradiation in Prostate Cancer: A Dosimetric Comparison. *Int. J. Part. Ther.* **2019**, *5*, 11–23. [[CrossRef](#)]
22. Santos, P.M.G.; Barsky, A.R.; Hwang, W.T.; Deville, C.; Wang, X.; Both, S.; Bekelman, J.E.; Christodouleas, J.P.; Vapiwala, N. Comparative toxicity outcomes of proton-beam therapy versus intensity-modulated radiotherapy for prostate cancer in the postoperative setting. *Cancer* **2019**, *125*, 4278–4293. [[CrossRef](#)] [[PubMed](#)]
23. Gogineni, E.; Cruickshank, I.K.; Chen, H.; Halthore, A.; Li, H.; Deville, C. In silico comparison of whole pelvis intensity-modulated photon versus proton therapy for the postoperative management of prostate cancer. *Acta Oncol.* **2023**, *62*, 642–647. [[CrossRef](#)] [[PubMed](#)]
24. Hall, W.A.; Paulson, E.; Davis, B.J.; Spratt, D.E.; Morgan, T.M.; Dearnaley, D.; Tree, A.C.; Efstathiou, J.A.; Harisinghani, M.; Jani, A.B.; et al. NRG Oncology Updated International Consensus Atlas on Pelvic Lymph Node Volumes for Intact and Postoperative Prostate Cancer. *Int. J. Radiat. Oncol. Biol. Phys.* **2021**, *109*, 174–185. [[CrossRef](#)] [[PubMed](#)]
25. Meyer, J.; Bluett, J.; Amos, R.; Levy, L.; Choi, S.; Nguyen, Q.N.; Zhu, X.R.; Gillin, M.; Lee, A. Spot scanning proton beam therapy for prostate cancer: Treatment planning technique and analysis of consequences of rotational and translational alignment errors. *Int. J. Radiat. Oncol. Biol. Phys.* **2010**, *78*, 428–434. [[CrossRef](#)] [[PubMed](#)]
26. Kirk, M.L.; Tang, S.; Zhai, H.; Vapiwala, N.; Deville, C.; James, P.; Bekelman, J.E.; Christodouleas, J.P.; Tochner, Z.; Both, S. Comparison of prostate proton treatment planning technique, interfraction robustness, and analysis of single-field treatment feasibility. *Pract. Radiat. Oncol.* **2015**, *5*, 99–105. [[CrossRef](#)] [[PubMed](#)]
27. Fang, P.; Mick, R.; Deville, C.; Both, S.; Bekelman, J.E.; Christodouleas, J.P.; Guzzo, T.J.; Tochner, Z.; Hahn, S.M.; Vapiwala, N. A case-matched study of toxicity outcomes after proton therapy and intensity-modulated radiation therapy for prostate cancer. *Cancer* **2015**, *121*, 1118–1127. [[CrossRef](#)] [[PubMed](#)]
28. Tang, S.; Both, S.; Bentefour, H.; Paly, J.J.; Tochner, Z.; Efstathiou, J.; Lu, H.M. Improvement of prostate treatment by anterior proton fields. *Int. J. Radiat. Oncol. Biol. Phys.* **2012**, *83*, 408–418. [[CrossRef](#)] [[PubMed](#)]
29. Underwood, T.; Giantsoudi, D.; Moteabbed, M.; Zietman, A.; Efstathiou, J.; Paganetti, H.; Lu, H.M. Can We Advance Proton Therapy for Prostate? Considering Alternative Beam Angles and Relative Biological Effectiveness Variations When Comparing Against Intensity Modulated Radiation Therapy. *Int. J. Radiat. Oncol. Biol. Phys.* **2016**, *95*, 454–464. [[CrossRef](#)] [[PubMed](#)]
30. Chera, B.S.; Vargas, C.; Morris, C.G.; Louis, D.; Flampouri, S.; Yeung, D.; Duvvuri, S.; Li, Z.; Mendenhall, N.P. Dosimetric study of pelvic proton radiotherapy for high-risk prostate cancer. *Int. J. Radiat. Oncol. Biol. Phys.* **2009**, *75*, 994–1002. [[CrossRef](#)]
31. Kuban, D.A.; Tucker, S.L.; Dong, L.; Starkschall, G.; Huang, E.H.; Cheung, M.R.; Lee, A.K.; Pollack, A. Long-term results of the M. D. Anderson randomized dose-escalation trial for prostate cancer. *Int. J. Radiat. Oncol. Biol. Phys.* **2008**, *70*, 67–74. [[CrossRef](#)]
32. Tucker, S.L.; Cheung, R.; Dong, L.; Liu, H.H.; Thames, H.D.; Huang, E.H.; Kuban, D.; Mohan, R. Dose-volume response analyses of late rectal bleeding after radiotherapy for prostate cancer. *Int. J. Radiat. Oncol. Biol. Phys.* **2004**, *59*, 353–365. [[CrossRef](#)] [[PubMed](#)]

33. Huang, E.H.; Pollack, A.; Levy, L.; Starkschall, G.; Dong, L.; Rosen, I.; Kuban, D.A. Late rectal toxicity: Dose-volume effects of conformal radiotherapy for prostate cancer. *Int. J. Radiat. Oncol. Biol. Phys.* **2002**, *54*, 1314–1321. [[CrossRef](#)]
34. Deville, C.; Jain, A.; Hwang, W.T.; Woodhouse, K.D.; Both, S.; Wang, S.; Gabriel, P.E.; Christodouleas, J.P.; Bekelman, J.; Tochner, Z.; et al. Initial report of the genitourinary and gastrointestinal toxicity of post-prostatectomy proton therapy for prostate cancer patients undergoing adjuvant or salvage radiotherapy. *Acta Oncol.* **2018**, *57*, 1506–1514. [[CrossRef](#)]
35. Kavanagh, B.D.; Pan, C.C.; Dawson, L.A.; Das, S.K.; Li, X.A.; Ten Haken, R.K.; Miften, M. Radiation dose-volume effects in the stomach and small bowel. *Int. J. Radiat. Oncol. Biol. Phys.* **2010**, *76*, S101–S107. [[CrossRef](#)]
36. Bryant, C.; Smith, T.L.; Henderson, R.H.; Hoppe, B.S.; Mendenhall, W.M.; Nichols, R.C.; Morris, C.G.; Williams, C.R.; Su, Z.; Li, Z.; et al. Five-Year Biochemical Results, Toxicity, and Patient-Reported Quality of Life After Delivery of Dose-Escalated Image Guided Proton Therapy for Prostate Cancer. *Int. J. Radiat. Oncol. Biol. Phys.* **2016**, *95*, 422–434. [[CrossRef](#)]
37. Yoon, M.; Kim, D.; Shin, D.H.; Park, S.Y.; Lee, S.B.; Kim, D.Y.; Kim, J.Y.; Pyo, H.R.; Cho, K.H. Inter- and intrafractional movement-induced dose reduction of prostate target volume in proton beam treatment. *Int. J. Radiat. Oncol. Biol. Phys.* **2008**, *71*, 1091–1102. [[CrossRef](#)]
38. Yoon, M.; Shin, D.; Kwak, J.; Park, S.; Lim, Y.K.; Kim, D.; Park, S.Y.; Lee, S.B.; Shin, K.H.; Kim, T.H.; et al. Characteristics of movement-induced dose reduction in target volume: A comparison between photon and proton beam treatment. *Med. Dosim.* **2009**, *34*, 191–201. [[CrossRef](#)]
39. Trofimov, A.; Nguyen, P.L.; Efstathiou, J.A.; Wang, Y.; Lu, H.M.; Engelsman, M.; Merrick, S.; Cheng, C.W.; Wong, J.R.; Zietman, A.L. Interfractional variations in the setup of pelvic bony anatomy and soft tissue, and their implications on the delivery of proton therapy for localized prostate cancer. *Int. J. Radiat. Oncol. Biol. Phys.* **2011**, *80*, 928–937. [[CrossRef](#)]
40. Soukup, M.; Söhn, M.; Yan, D.; Liang, J.; Alber, M. Study of robustness of IMPT and IMRT for prostate cancer against organ movement. *Int. J. Radiat. Oncol. Biol. Phys.* **2009**, *75*, 941–949. [[CrossRef](#)] [[PubMed](#)]
41. Wang, Y.; Efstathiou, J.A.; Sharp, G.C.; Lu, H.M.; Ciernik, I.F.; Trofimov, A.V. Evaluation of the dosimetric impact of interfractional anatomical variations on prostate proton therapy using daily in-room CT images. *Med. Phys.* **2011**, *38*, 4623–4633. [[CrossRef](#)] [[PubMed](#)]
42. Thomas, R.; Chen, H.; Gogineni, E.; Halthore, A.; Floreza, B.; Esho-Voltaire, T.; Weaver, A.; Alcorn, S.; Ladra, M.; Li, H.; et al. Comparing Ultra-hypofractionated Proton versus Photon Therapy in Extremity Soft Tissue Sarcoma. *Int. J. Part. Ther.* **2023**, *9*, 30–39. [[CrossRef](#)]
43. Vargas, C.; Fryer, A.; Mahajan, C.; Indelicato, D.; Horne, D.; Chellini, A.; McKenzie, C.; Lawlor, P.; Henderson, R.; Li, Z.; et al. Dose-volume comparison of proton therapy and intensity-modulated radiotherapy for prostate cancer. *Int. J. Radiat. Oncol. Biol. Phys.* **2008**, *70*, 744–751. [[CrossRef](#)]
44. Veas, H.; Dipasquale, G.; Nouet, P.; Zilli, T.; Cozzi, L.; Miralbell, R. Pelvic Lymph Node Irradiation Including Pararectal Sentinel Nodes for Prostate Cancer Patients: Treatment Optimization Comparing Intensity Modulated X-rays, Volumetric Modulated Arc Therapy, and Intensity Modulated Proton Therapy. *Technol. Cancer Res. Treat.* **2015**, *14*, 181–189. [[CrossRef](#)]
45. Widesott, L.; Pierelli, A.; Fiorino, C.; Lomax, A.J.; Amichetti, M.; Cozzarini, C.; Soukup, M.; Schneider, R.; Hug, E.; Di Muzio, N.; et al. Helical tomotherapy vs. intensity-modulated proton therapy for whole pelvis irradiation in high-risk prostate cancer patients: Dosimetric, normal tissue complication probability, and generalized equivalent uniform dose analysis. *Int. J. Radiat. Oncol. Biol. Phys.* **2011**, *80*, 1589–1600. [[CrossRef](#)]

Disclaimer/Publisher’s Note: The statements, opinions and data contained in all publications are solely those of the individual author(s) and contributor(s) and not of MDPI and/or the editor(s). MDPI and/or the editor(s) disclaim responsibility for any injury to people or property resulting from any ideas, methods, instructions or products referred to in the content.